

Collective incentives reduce over-exploitation of social information in unconstrained human groups

Dominik Deffner^{1,2*}, David Mezey^{2,3}, Benjamin Kahl¹, Alexander Schakowski¹, Paweł Romanczuk^{2,3}, Charley M. Wu^{1,4,5} & Ralf H.J.M. Kurvers^{1,2}

¹Center for Adaptive Rationality, Max Planck Institute for Human Development, Berlin, Germany

²Science of Intelligence Excellence Cluster, Technical University Berlin, Berlin, Germany

³Institute for Theoretical Biology, Humboldt University Berlin, Berlin, Germany

⁴University of Tübingen, Tübingen, Germany

⁵Max Planck Institute for Biological Cybernetics, Tübingen, Germany

*deffner@mpib-berlin.mpg.de

ABSTRACT

Collective dynamics emerge from countless individual decisions. Yet, we poorly understand the cognitive processes governing dynamically-interacting individuals in human collectives under realistic conditions. We present a naturalistic immersive-reality experiment where groups of participants searched for rewards in different environments, studying how individuals weigh personal and social information and how this shapes individual and collective outcomes. Capturing high-resolution visual-spatial data, behavioral analyses revealed individual-level gains—but group-level losses—of high social information use and spatial proximity in environments with concentrated (vs. distributed) resources. Incentivizing participants at the group (vs. individual) level facilitated adaptation to concentrated environments, buffering excessive scrounging. To infer discrete choices from unconstrained interactions and uncover the underlying decision mechanisms, we developed an unsupervised Social Hidden Markov Decision model. Computational results showed that participants were more sensitive to social information in concentrated environments frequently switching to a ‘social relocation’ state where they approach successful group members. Group-level incentives reduced participants’ overall responsiveness to social information and promoted higher selectivity over time. Finally, mapping group-level spatio-temporal dynamics through time-lagged regressions revealed a collective exploration-exploitation trade-off across different timescales. Our study unravels the processes linking individual-level strategies to emerging collective dynamics, and provides new tools to investigate decision-making in freely-interacting collectives.

Key words. Social information use, decision-making, collective dynamics, Hidden Markov models, social learning

1. Introduction

Collective behavior emerges from individual-level cognition, and the cognitive mechanisms driving social interactions strongly determine whether social influence

5 promotes adaptive behavior or leads to maladaptive herding [1, 2]. Despite their crucial role in governing the outcomes of collective behaviors, the cognitive processes of human collectives under naturalistic conditions remain poorly understood [3, 4].

10 One of the key trade-offs driving collective systems is between using personal versus social information. Relying too heavily on personal information prevents the spread of useful information, while relying too heavily on social information reduces exploration and generates over-exploitation of the environment [5–9]. This trade-off is key across social contexts, from social foraging [10], to the discovery of new tools [11, 12], or computer code [13], to the planting of crops [14, 15].

In all such situations, individuals must continuously integrate their personal information with information acquired from others and make strategic decisions on different timescales. The cognitive underpinnings of these processes are, however, still largely unknown.

20 Most experimental studies to date on social decision-making used static—and often simulated—sources of social information [7] or let interacting participants choose among a small set of well-defined options at prespecified time points [e.g., 14–18]. To understand the mechanisms governing real-world human collective systems, we need paradigms that allow complex social dynamics to unfold within naturalistic environments. Analyzing behavior in such complex systems requires novel computational models that describe how dynamically-interacting individuals make decisions while accounting for their unique (visual) perspectives and spatial constraints [2, 19, 20].

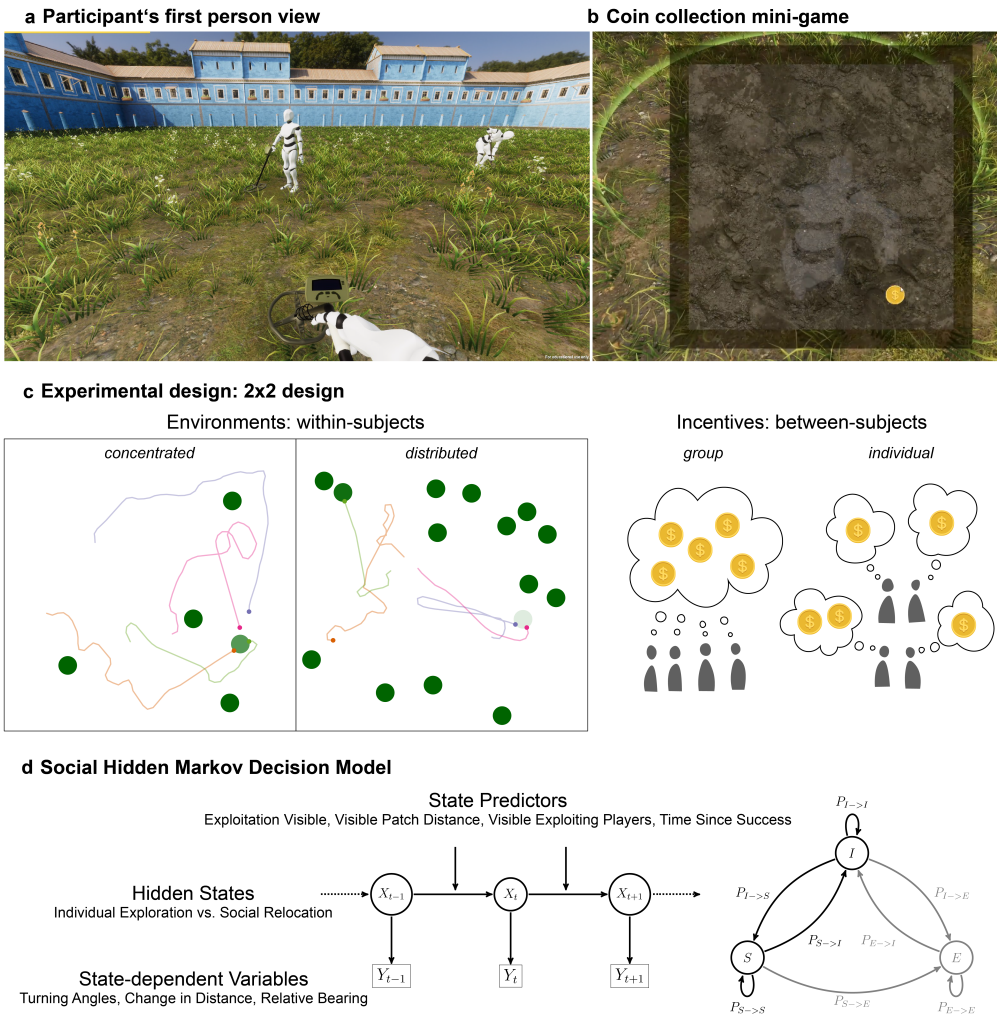


Fig. 1: Collective foraging task and Social Hidden Markov Decision model. (a) Participants in groups of four searched for circular research patches in a square environment. A metal detector lighted up when they have discovered a patch. Participants could observe each other in real time and decide to join other players who have discovered a patch (exploiting players indicated by digging animation; see avatar on the right). (b) Once participants have discovered a patch or joined others, they started extracting coins in a mini-game by clicking on coin symbols appearing on the screen in a 2-second interval. (c) Participants completed four rounds of the task in a 2x2 experimental design. Each group conducted two rounds in a *concentrated* environment (5 patches with 48 coins each) and two rounds in a *distributed* environment (15 patches with 16 coins each). Colored dots and lines represent snapshots of the current position of four players as well as their movement trajectories in the last minute. Lighter green patches have fewer coins left. Half of the groups were incentivized on the *group* level and half of the groups were incentivized on the *individual* level. (d) Our computational approach uses state-dependent variables to assign participants to hidden states at each time point: “Individual Exploration” (I ; independently search for resource patches) or “Social Relocation” (S ; use social information and approach successful group members). The model simultaneously infers the transition probabilities between latent states (as E is known, we only need to explicitly model transitions between I and S). We model the (time-dependent) influence of state predictors on the probability to stop exploring and switch to social relocation, $P_{I \rightarrow S}$ (see Eq. 1).

Here, we use an immersive-reality approach to study how groups of four participants search for resources (“coins”) in a 3D virtual environment with different resource distributions and incentive structures. Participants could observe each other in real time and decide to join players who successfully discovered a resource patch (Fig. 1a; video S1). The 3D environment

imposes a limited, first-person, field of view as well as realistic spatial constraints creating a natural trade-off between individual exploration of the environment and social information use [20, 21]. Participants completed four rounds of the task in a 2x2 design (Fig. 1c; see Methods). In half of the rounds, resource units were *concentrated* in relatively few—but rich—patches. In

the other rounds, the same number of units were *distributed* among many—but poorer—patches. Theory on producer-scrounger games [e.g., 5, 10, 22–25] predicts that a “scrounging” strategy, where agents use social information to join resource patches discovered by others, increases in frequency (relative to individually-searching “producers”) when patches are difficult to find but rich in resources. Therefore, we expected participants to rely more on social information and to be less selective in concentrated compared to distributed environments.

Across social systems, individual incentives do not always align with the interest of the collective and theory on producer-scrounger dynamics [5, 10, 23–25], and the evolution of social learning [6, 26] predicts that social information use can be individually beneficial while reducing collective performance or population fitness. To investigate how participants balance the pros and cons of social information use depending on their interdependence with others, half of the groups were incentivized on the group level (i.e., paid depending on group success), while the other half on the individual level (i.e., paid depending on personal success). Since scroungers capitalize on others’ discoveries and compete for limited local resources, we expected participants to rely less on social information when incentivized on the group level reducing maladaptive over-exploitation of social information (see preregistration for the full set of predictions: <https://osf.io/5r736/>).

Our analyses leveraged high-resolution time-series data from each participant of their visual information and movement trajectories. Behavioral analyses revealed individual-level benefits of high social information use and spatial proximity in concentrated resource environments, which came at the expense of group performance. Crucially, group-level incentives alleviated the negative consequences of excessive scrounging. We next developed an unsupervised *Social Hidden Markov Decision model* (inspired by animal movement models in ecology [27, 28]) to simultaneously infer decision sequences between latent states and describe how resource distributions, incentives, and situational factors influence participants’ decisions to use social information (Fig. 1d). Quantifying such latent social decision-making, we uncovered the mechanisms underlying behavioral outcomes, demonstrating how participants strategically adjusted their social information use to both environmental demands and incentive structure. Group incentives facilitated adaptive tuning of decision strategies over time, with increased selectivity acting as a safeguard against maladaptive over-reliance on social information. Finally, we mapped the emerging group-level spatio-temporal dynamics through time-lagged Gaussian process regressions and discovered consistent collective benefits of more individualistic search in distributed environments and a collective exploration-exploitation trade-off in concentrated environments.

2. Results

We start by examining participants’ behavior before turning to computational analyses. Results are reported as population-level effects from hierarchical Bayesian models controlling for participant- and group-level variability in both intercepts and slopes. Inferences are based on posterior contrasts between conditions (on the outcome scale for behavior, on a latent scale for computational results), reported as posterior means and 90% highest posterior density intervals (HPDIs).

Foraging performance and scrounging

Participants incentivized on the group level showed no difference in performance between environments (-0.05 [-8.9,8.1]; Fig. 2a), whereas participants incentivized on the individual level performed worse in concentrated than distributed environments (-8.4 [-16.7, -0.5]). To quantify success differences among incentive conditions over time, we computed exploitation probabilities at one minute intervals in each round (Fig. 2b; Fig. S1). In concentrated environments, group-incentivized participants consistently outperformed those incentivized on the individual level after four minutes. In distributed environments, individually-incentivized participants initially performed better before converging on the same probability of success.

The structure of the environment also induced different patterns of foraging behavior. In concentrated environments, participants discovered fewer new patches (group incentives: -5.2 [-5.7,-4.7]; individual incentives: -5.6 [-6.1,-5.1]) but joined more patches discovered by others (group incentives: 1.4 [0.7,2]; individual incentives: 1.1 [0.4,1.8]). Participants also stayed closer to group members (average distance to the other three players when focal player was not exploiting; group incentives: -6.4 [-7.6, -5.3]; individual incentives: -8.8 [-10.1, -7.6]) and looked more at others (average number of players in field of view when focal player was not exploiting; group incentives: 0.08 [0.05,0.1]; individual incentives: 0.14 [0.11,0.17]; see Fig. S2), suggesting increased social attention in concentrated environments (see Fig. S3 for aggregated results).

To account for the influence of participants’ unique visual perspectives, we next computed scrounging rates as conditional probabilities for players to join a patch where they had observed one (or more) exploiting group member(s). Scrounging rates were higher in concentrated than in distributed environments (group incentives: 0.44 [0.37,0.50]; individual incentives: 0.48 [0.42,0.54]), with most scrounging behavior occurring in participants incentivized on the individual level while foraging in concentrated environments (Fig. 2c).

Determinants of individual and collective success

Can excessive scrounging explain the reduced performance of individually-incentivized participants in con-

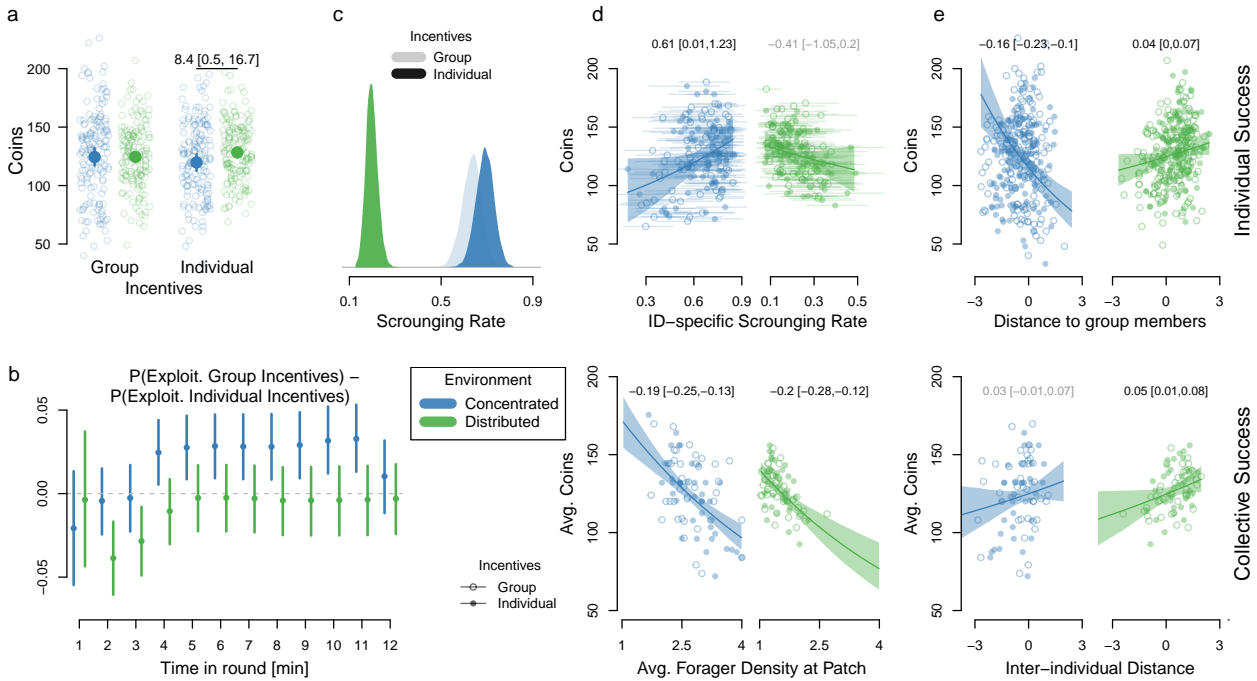


Fig. 2: Behavioral Results. (a) Coins collected per incentive condition and environment. Each circle represents one round per participant, larger filled dots represent posterior estimates (as well as 90% HPDIs) from a Bayesian multilevel Poisson model. (b) Performance differences between incentive conditions (positive values indicate an advantage for group incentives), computed as the probability of exploiting a patch in one minute intervals. (c) Posterior scrounging rates (conditional probabilities that players join a patch where they had observed at least one exploiting group member) per incentive condition and environment. (d) Average number of coins collected per individual as a function of individual-specific scrounging rates (with 90% HPDIs; top) and per group as a function of forager density (i.e., average number of players exploiting a given patch; bottom). (e) (Average) number of coins per round per individual (top) and group (bottom) in concentrated and distributed environments as a function of distance (standardized average distance to other players). Lines and uncertainty intervals show effects from multilevel regressions accounting for baseline differences between incentive conditions and individual- and group-level variability in both intercepts and slopes (transparent text if 90% HPDI overlaps 0).

centrated environments? To relate behavioral metrics to the number of collected coins, we used multilevel Poisson regressions accounting for baseline success differences between incentive conditions. In concentrated environments, individual participants benefited from high scrounging rates (Fig. 2d, top) and close proximity to others (Fig. 2e, top). This confirms individual-level adaptive benefits of social information use in resource environments where the behavior of others provides valuable information. By contrast, collective performance was higher if, on average, fewer players exploited a patch (Fig. 2d, bottom) and group members kept greater inter-individual distance (Fig. 2e, bottom), revealing opposing effects of social information use on individual vs. collective performance. In distributed environments, where social information has lower value, both individual and collective performance was highest if participants joined fewer patches discovered by group members and stayed further away from each other.

Beyond social information use, participants also collected more coins if they independently discovered more new patches in both concentrated (0.14

[0.12, 0.15]) and distributed (0.09 [0.08, 0.09]) environments as patch discoverers had more time to collect coins without sharing resources with others. For both environments, participants with relatively directed and regular movement trajectories discovered more patches highlighting an important role for effective individual search (Fig. S4).

Solitary foragers

To compare group foragers to solitary ones, we recruited additional participants who searched for coins on their own (see Methods). Foraging in the same resource environments but without competition, individual foragers, on average, collected more coins than participants in groups. They performed similarly in both environments and discovered more patches in distributed environments (Fig. S5; see Fig. S6 for movement metrics and discoveries).

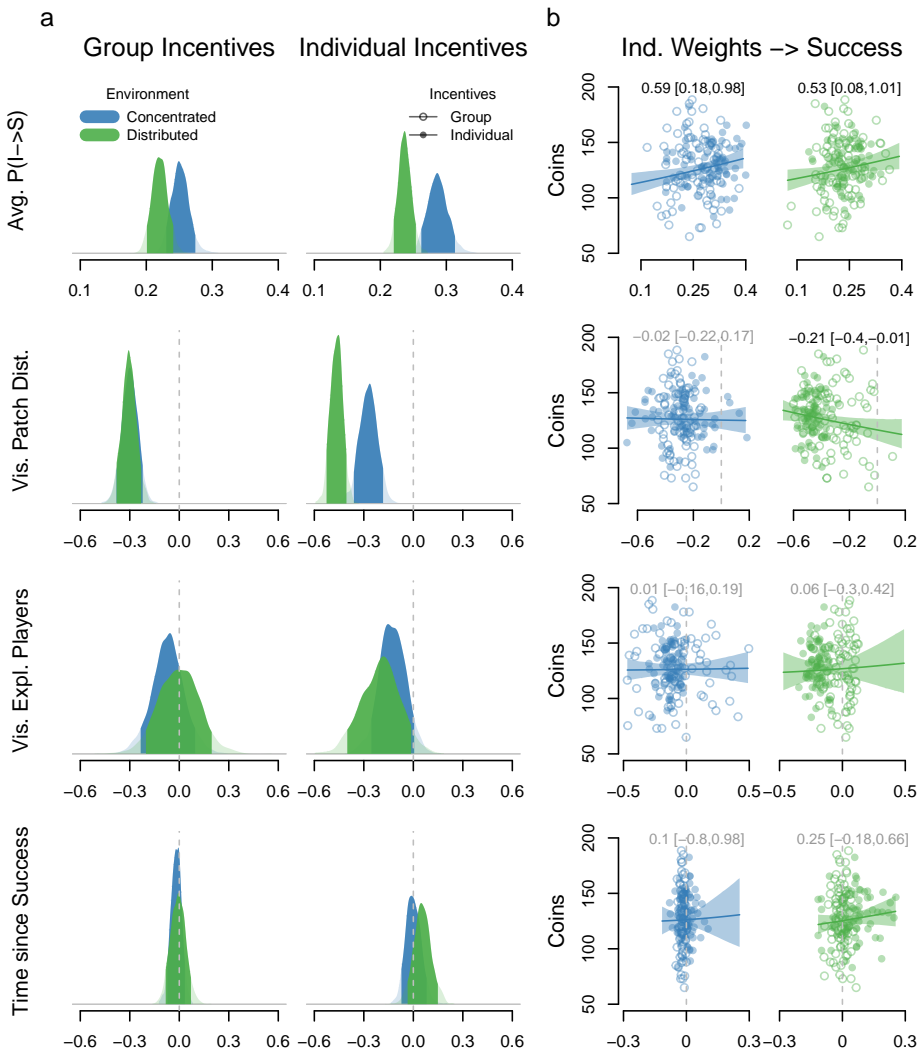


Fig. 3: State predictors and their adaptive consequences (a) Full posterior distributions (transparent curves) and 90% HPDIs (darker areas) for the influence of different state predictors on the probability that participants switch from individual exploration to social relocation per environment and incentive condition. The top row shows baseline switching probabilities across all situations in which participants observe (a) successful player(s), the other rows show deviations from this expectation on the logit scale. (b) Success (average number of coins collected per individual) in concentrated (left) and distributed (right) environments as a function of individual-level decision weights. Lines and uncertainty intervals show effects from log-normal regression models accounting for baseline success differences between incentive conditions (reported above, transparent text if 90% HPDI overlaps 0).

Social Hidden Markov Decision Model

Next, we use a computational approach to delineate the cognitive mechanisms underlying participants' decisions to respond to or ignore social information. A computational approach is necessary because observable metrics, such as patch joining events, are only indirect indicators of underlying processes [29]. Imagine, for instance, that a player decides to use social information and moves towards an exploiting group member but does not arrive before all coins are collected; or, more luckily, this player might even independently discover a new patch while relocating. In both scenarios,

we do not observe the player joining a patch, although they have actively decided to use social information.

Our model uses time series of three state-dependent variables (on a one-second resolution; Fig. 1d and Fig. S7) to probabilistically assign participants to one of two latent states at each point in time: *individual exploration* or *social relocation* (see Methods). Individual exploration is characterized by irregular movement not directed towards successful peers, whereas social relocation is characterized by consistent, directed movement towards exploiting group members. Note that the latent states are statistically inferred from changes

205
210
215
220

225 in movement and interaction patterns, not hard-coded
 based on arbitrary criteria. Reassuringly, the model es-
 timated smaller turning angles, larger reduction in dis-
 tance to exploiting players and smaller relative bear-
 230 ings for the social relocation state compared to the in-
 dividual exploration state (Fig. S8), confirming that the
 identified latent states correspond to our target of inference
 235 (Fig. S7 shows an example of a recovered state se-
 quence using the Viterbi algorithm).

State predictors and their adaptive consequences

240 Our model simultaneously infers the time-dependent
 transition probabilities between latent states. This al-
 lows us to describe how incentive conditions i and re-
 source distributions j along with currently available (vi-
 245 sual) information influence the probability of switching
 from individual exploration to social relocation at time
 t . Specifically, we estimated the condition-specific in-
 fluence of exploitation visibility V , visible patch dis-
 tance D , number of visible exploiting players N , and
 250 time since success T (Fig. 1d; see Methods) :

$$P_{I \rightarrow S_t} = \text{logit}^{-1}(\alpha_{ij[t]} + \beta_{V_{ij[t]}} V_t + \\ \beta_{D_{ij[t]}} D_t + \beta_{N_{ij[t]}} N_t + \beta_{T_{ij[t]}} T_t) \quad (1)$$

255 Averaging over all situations when at least one exploi-
 ting player was visible (i.e., $V = 1$), participants were
 more likely to switch to social relocation and approach
 others in concentrated compared to distributed environ-
 260 ments with both group (0.03 [0.004, 0.06]) and indi-
 vidual (0.05 [0.02, 0.08]) incentives (Fig. 3a, first row).
 Moreover, individual incentives reliably increased par-
 265 ticipants' propensity to use social information in con-
 centrated (0.04 [0.001, 0.07]) but not in distributed
 (0.01 [-0.01, 0.04]) environments. Thus, participants
 270 were more likely to switch to social relocation when
 prioritizing their individual success, particularly in con-
 centrated environments where scrounging is beneficial,
 uncovering the decision mechanisms underlying the
 275 observed scrounging rates (Fig. 2c). Using individual
 decision-weight estimates from the multilevel compu-
 tational model to predict success reveals that individ-
 uals benefited from more social information use in both
 environments (Fig. 3b, first row).

280 Turning to the strategies participants used to inte-
 grate social information, we found that, across condi-
 tions, participants were more likely to use social in-
 formation if observed successful group members were
 close rather than farther away, suggesting selective
 285 rather than indiscriminate use of social information
 (Fig. 3a, second row). This also proved adaptive as
 participants who were more selective with respect to
 distance were more successful in distributed, but not
 in concentrated environments (Fig. 3b, second row).
 290 Moreover, participants preferentially decided to join
 patches where fewer group members were exploiting
 in the individual but not in the group incentive condi-
 tion (Fig. 3a, third row). Being selective with respect to

the number of others at a patch proved neutral in both
 environments (Fig. 3b, third row), likely reflecting the
 fact that participants observed two players exploiting
 the same patch in only 14% of cases and three players
 295 in only 3% of cases (one player in 83%). As a last fac-
 tor, we also investigated the influence of past personal
 success on the probability to respond to social infor-
 mation. Surprisingly, we found that participants did not
 become more likely to use social information if unsuc-
 300 cessful for a longer time and there was also no relation-
 ship between individual-level weights and foraging
 success (Fig. 3a,b, fourth row).

Investigating the role of latent decision weights on
 collective performance confirms the same pattern ob-
 served for behavioral outcomes (Fig. S9). The aver-
 age baseline probability to turn social for groups was
 negatively related to collective success in concentrated
 environments, again revealing a striking contrast to
 individual-level outcomes where high social informa-
 tion use proved beneficial. Other decision weights were
 unrelated to collective success.

Temporal dynamics in state predictors

Over time, group-incentivized participants outper-
 formed those incentivized on the individual level in
 concentrated environments (Fig. 2b). Did participants
 adjust their decision-making over time or did they enter
 305 the experiment with fixed, unchanging strategies?
 Figure 4 shows the temporal dynamics in state predic-
 tors from the time-varying state predictors model (see
 Fig. S10 for similar linear trends).

We first focus on participants incentivized on the
 group level. Participants started with similar overall
 propensities for social information use in both envi-
 ronments but, over time, became more likely to use
 310 social information in concentrated (0.20 [-0.02, 0.42])
 and less likely to use social information in distributed
 environments (-0.11 [-0.27, 0.05]), suggesting adaptive
 calibration of social decision-making over time. Partic-
 ipants in concentrated environments started as rather
 315 indiscriminate social learners but, over time, became
 more selective and began to strongly rely on distance (-
 0.45 [-0.64, -0.26]) and the number of exploiting play-
 ers (-0.55 [-0.88, -0.24]) as cues. This tuning of deci-
 320 sion strategies towards more selectivity might act as a
 safeguard against the over-reliance on social informa-
 tion and, therefore, (partly) explain the emerging ben-
 efits of collectively-incentivized participants (Fig. 2b). In
 distributed environments, decision weights stayed rel-
 atively constant and there were no clear trends in the
 325 influence of the time since the last success.

In the individual incentive condition, baseline levels
 of social information use started at higher levels com-
 pared to the group incentive condition and increased
 even further in concentrated environments (0.18 [-
 0.03, 0.40]). Unlike collectively-incentivized partic-
 ipants, there was no distinct development towards more
 330 selective social information use in either environment.

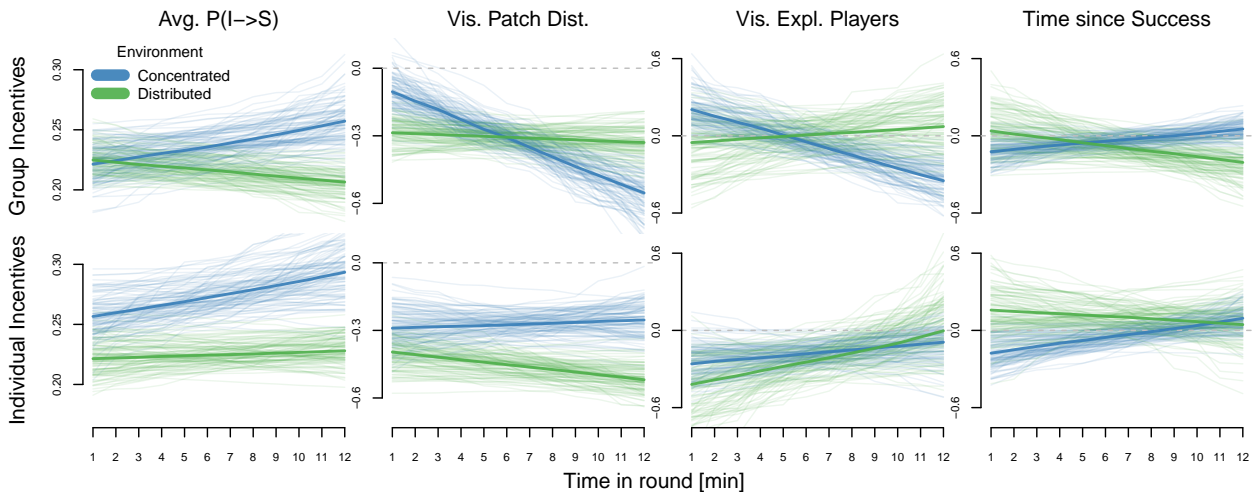


Fig. 4: Temporal dynamics in state predictors. 100 random draws from the posterior distribution (transparent lines) as well as posterior means (solid lines) for the influence of different state predictors over time in each round. The first column shows baseline switching probabilities across all situations in which participants observe (a) successful player(s), the following columns show deviations from this expectation on the logit scale.

335 Collective visual-spatial dynamics

Our behavioral results suggested that, overall, groups benefited from less social information use and lower proximity in both environments (Fig. 2d,e, bottom). Last, to better understand the more fine-grained collective dynamics, we quantify the changing relationships between groups' visual-spatial organization and collective foraging success for different time lags (Fig. 5; Fig. S11 shows results for up to 3-minute time lags in steps of 5 seconds). Positive (negative) regression weights for a given time lag τ mean that greater inter-individual distance/visibility among group members at time $t - \tau$ increased (decreased) groups' current collective foraging success at time t .

In distributed environments, groups of individuals who stayed farther away from each other were indeed more successful irrespective of time interval and incentive condition. In concentrated environments, we observed more intricate temporal dynamics. At relatively short timescales ($\approx 15s$ for group incentives, $\approx 8s$ for individual incentives), smaller inter-individual distances were associated with greater collective success; being closer together allowed collectives to better exploit clustered resources discovered by group members. This beneficial effect of grouping was especially pronounced for groups incentivized on the collective level. On the flip side, at longer timescales, larger distances among group members were associated with greater foraging success. If groups disperse, they are better able to explore large parts of the environment and discover one of the few, rich patches, thereby, increasing their collective foraging success in the future. Individually-incentivized groups benefited more strongly from spatial distancing, likely because their higher sensitivity

370 to social information increased their risks for over-exploitation and herding. At even longer timescales, there was no longer an association between group distance and foraging success (Fig. S11).

375 Turning to inter-individual visibility, we observe a strong negative effect at short timescales ($\approx 20s$) for both environments and incentive conditions. As players could not see others while exploiting a patch, low visibility often meant that a lot of players were currently collecting coins. More substantially, the number of visual connections among group members was positively related to collective success longer into the future across all conditions, suggesting that groups paying more attention to others in this crucial time window of patch discovery had greater success later on.

3. Discussion

385 Finding and collecting rewards in heterogeneous environments is key for adaptive collective behavior, yet it remains largely unknown how individuals in freely interacting groups make strategic choices in naturalistic environments and how these choices might shape individual and collective outcomes. We designed a 3D immersive-reality collective foraging paradigm to obtain fine-grained visual and spatial data from interacting groups and developed computational Social Hidden Markov Decision models to extract and understand strategic choices from naturalistic behavior. Collective foraging provides an ideal testbed to study social decision-making and collective adaptation in a controlled, yet ecologically-relevant, context [1, 30]. Anthropologists have identified our unique abilities to collectively find and extract high-quality resources from diverse environments as a defining feature of human

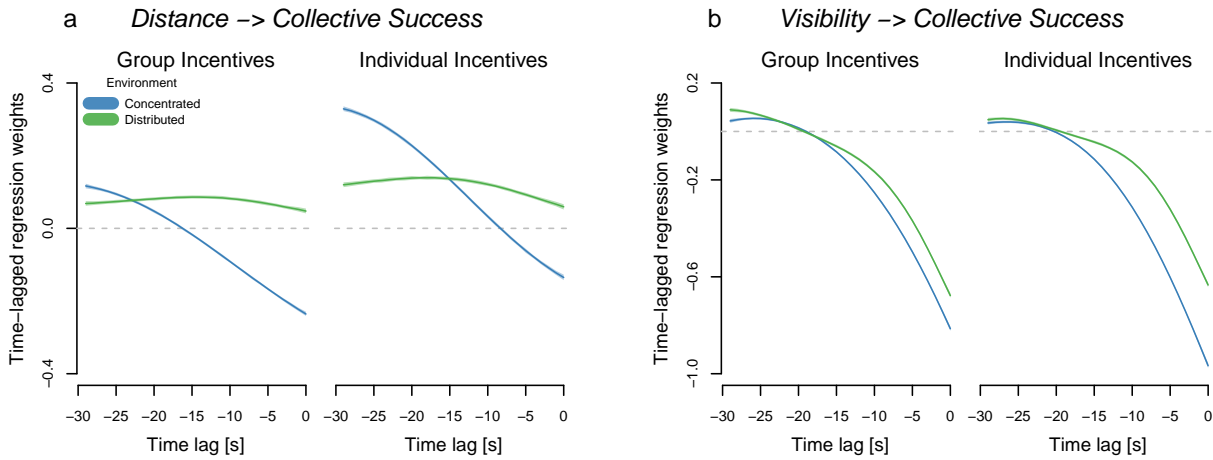


Fig. 5: Collective visual-spatial dynamics. Time-lagged Gaussian-process regression weights (including 90% HPDIs) predicting collective foraging success (number of players exploiting a patch) based on (a) distance (average pairwise distance among players) and (b) visibility (number of visual connections among group members, ranging from 0, where no one is looking at others, and 12, where everyone is looking at everyone else) across different time intervals per incentive condition and environment.

adaptability [31–34]. Collective foraging further unites several key ecological and social challenges, such as navigating uncertain environments, cooperating with others to achieve common goals, as well as competing to gain privileged access to resources [30, 35].

As predicted by theoretical models of collective foraging [e.g., 24, 36], participants systematically adjusted their social information use to the resource distribution relying more on the behavior of others when resources were difficult to find, but provided a large potential for exploitation (i.e., in concentrated compared to distributed environments). Moreover, participants adaptively calibrated their strategies over time, becoming more (less) likely to use social information in concentrated (distributed) environments, extending previous research highlighting the importance of selective and strategic social learning rather than pure copying or innovation [13, 15, 20].

In both environments, individuals benefited from high propensities to switch to social relocation, whereas actually capitalizing on social information and scrounging at patches discovered by others was only adaptive in concentrated environments but maladaptive in distributed environments. Participants could still discover new patches while approaching group members and more directed movement even generally increased their chances of patch discovery. Therefore, participants incurred little costs by frequently responding to social information even if resources were evenly distributed, thus generating divergent consequences for latent propensities to respond to social information compared to manifest outcomes. Moreover, in distributed environments, where far-away patches were likely depleted before arrival, participants collected more points if they tuned their propensity to switch to social relocation based on the distance of exploiting group members,

confirming recent theoretical predictions on the importance of selective copying in collective search [37].

Strikingly, large amounts of social information use proved adaptive for individuals (in concentrated environments) but maladaptive for collectives. Groups performed better in either environment if, on average, fewer players exploited a given patch and players stayed further away from each other; additionally, solitary foragers generally outperformed participants in groups. However, placing the incentives on the collective level alleviated the negative collective consequences of high social information use. In concentrated environments, where scrounging is individually beneficial, collectively-incentivized participants were less likely to respond to social information and exploit patches discovered by others, increasing their foraging success compared to participants incentivized on the individual level. Group incentives also facilitated adaptive tuning of latent decision strategies over time, with increased selectivity safeguarding against maladaptive over-use of social information.

These pervasive collective drawbacks of high social information use seem to contradict models of collective search [e.g., 36–38] that have shown that high degrees of social information use can also be beneficial on a collective level in rich and clustered environments. However, in such models, individual exploration is typically governed by a random walk or similar stochastic process and social information provides the only source of adaptive information. Human participants, in contrast, use rich internal models of the environment and the task, as well as memory, to systematically search the arena. These enhanced individual exploration abilities likely shifted the relative collective benefits of personal and social information use compared to theoretical models.

Moreover, our time-lagged dynamics analysis provided a subtler picture of when and how it was beneficial for collectives to join forces. In distributed environments, collectives indeed consistently benefited from independent search of the arena. Concentrated environments revealed an intricate trade-off between collective exploration and exploitation. While close spatial proximity allowed groups to efficiently exploit discovered patches, at longer timescales, collectives benefited from larger inter-individual distances which facilitate new patch discoveries and increase foraging success in the future. Therefore, if resources are difficult to find but provide a large potential for exploitation, collective foragers need to dynamically adjust their visual-spatial organization over time and collectively strike the right balance between independent exploration and joint exploitation. A promising avenue for future research could be to investigate cases of collective foraging where social information use does not create zero-sum scenarios as in the present paradigm but facilitates novel adaptive abilities to emerge on the group level such as collective tracking of mobile resources [39–41].

To identify and model latent choices between different behavioral states (“Individual Exploration” and “Social Relocation”), we developed a novel Social Hidden Markov Decision model. Traditionally, cognitive and behavioral scientists have investigated choices in relatively static and highly standardized experimental situations. Although abstracting away from real-world details and controlling the environment participants face can allow researchers to more accurately identify cognitive processes and strategies, ultimately, we aim to understand how people make unconstrained decisions in relevant real-world ecologies. Technological advances now provide us with unprecedented access to the individual-level informational environments and constraints that guide strategic choices in humans and other animals [20, 42, 43]. Such dynamic data require dynamic statistical inference and Hidden Markov models provide ideal tools to simultaneously extract meaningful patterns from multidimensional time-series data and use internal or external situational factors to predict switches between the identified hidden states. Although our model is tailored to the present experimental paradigm (especially with respect to the state-dependent variables), our freely available modeling code and in-depth documentation set the scene for future research on the socioecological drivers of dynamic social decision-making in human and (non-human) animal collectives. In addition to other naturalistic behavioral experiments [20, 44, 45], Social Hidden Markov Decision models can, for instance, be applied to human crowd behavior to better understand how situational factors influence movement patterns and potentially cause stampedes [46, 47]; they can be adapted to sports analytics where Hidden Markov models have already been used to identify drive events and defensive assignments in basketball [48, 49] or “hot hands” in darts [50]; they could elucidate dynamic leader-follower dynamics

in animal societies and help us better understand when and why animals follow the example of others [51, 52]; and they could be applied to GPS data from subsistence foragers [53, 54], cell phone users [55, 56] or migratory animals [57–59] to infer modes of (collective) search, movement and space use across different spatial and temporal scales.

In summary, our work mechanistically links individual-level social information use to collective dynamics in naturalistic interactions. Through behavioral and computational analyses, we have demonstrated how group incentives can improve collective performance by reducing individually beneficial, but collectively costly, exploitation of social information. Maybe most importantly, this work showcases a novel way of studying human behavior that goes beyond the often highly constrained experiments of psychology, economics, and cognitive science, moving towards a science of unconstrained behavior that dynamically unfolds in naturalistic and socially interactive environments.

4. Methods

Participants

160 participants were recruited from the Max Planck Institute for Human Development (MPIB) recruitment pool and invited in anonymous groups of four to the behavioral laboratory at the MPIB in Berlin, Germany (63 identified as male, 97 as female; $M_{age} = 28.5$, $SD_{age} = 6.4$ years; all were proficient in German and most came from Western, educated, industrialized, rich, and democratic societies [60, 61]). 40 additional participants were recruited for an individual control condition (14 identified as male, 26 as female; $M_{age} = 29.8$, $SD_{age} = 5.7$ years). The study was approved by the Institutional Review Board of the MPIB (number: A 2022-06) and participants signed an informed consent form prior to participation. Participants received a base payment of €18 plus a bonus of €0.01 per coin (depending on incentive condition, see below), earning on average $\text{€}23.09 \pm 0.71$ (SD) for a total time of about one hour.

Procedure

Participants started with an in-game tutorial to familiarize themselves with the keys and virtual environment (see video S2). Participants then completed the task in groups of four, interacting live in a 3D immersive game environment. Group members were seated in the same room; opaque desk divider panels ensured that they could not observe each other’s screen and mice with silent buttons prevented them from hearing when others clicked on coins during the coin collection mini-game. Over four rounds lasting twelve minutes each, participants controlled avatars in the virtual world (a square 90m x 90m “castle courtyard”) and searched for resources (“coins”) hidden under ground (Fig. 1a; video S1). At the beginning of each round, a fixed number (see section below) of non-overlapping circular resource patches (“coin fields”) with a radius of $r = 3$ meters was randomly placed across the arena. Participants used keyboard buttons to freely navigate through the virtual environment and detect resource patches with a metal detector. Participants could only move their avatar for-

590 ward, turn right or turn left using the “W”, “A” and “D” keys, respectively. All other keys were deactivated.

When individuals encountered a patch, their metal detector lighted up and they could start collecting coins by clicking on coin symbols appearing at different locations on the screen (Fig. 1b). New coins appeared at a fixed interval of two seconds and stayed on the screen until collected (this interval was chosen as pilots showed that all participants were able to collect coins within two seconds). This simple “mini game” ensured that participants stayed engaged throughout the experiment without introducing additional sources of variation in performance. Participants continued collecting coins at a patch (and, therefore, could not move) until it was depleted. After that, the patch disappeared and a new patch containing the same number of coins was generated at a random location in the environment (ensuring that it did not overlap with any existing patch or participant). This means the number of patches and, therefore, the task structure remained constant within each round avoiding any effects of resource depletion or diminishing returns.

In addition to individual exploration of the environment, participants could also observe the behavior of others and freely decide to join players who have successfully discovered a resource patch. Avatars in the virtual environment performed a digging movement using a shovel to indicate that they were currently extracting coins (right avatar in Fig. 1a). If multiple players simultaneously collected coins from the same patch, each player extracted coins at the same rate of one coin every two seconds and coins, therefore, disappeared from a patch at a rate proportional to the number of extracting players. This means there was exploitative, but not interference, competition among players.

The 3D virtual environment imposed a limited, first-person, field of view (108° horizontal and 76° vertical FOV) as well as realistic spatial constraints (maximum movement speed of 2 m/s) creating natural trade-offs between individual exploration of the environment and social information use [20, 21]. The experiment was implemented using the *Unity* [62] game engine (version 2020.3.21 [63], built-in rendering pipeline) with the Netcode for GameObjects and Unity Transport libraries for networking functionality. The four instances for participants were connected to a local Windows Server running a Server Build of the experiment with a tick rate of 25Hz. Player movement was handled client-side.

Experimental Design

The experiment followed a 2x2 design (Fig. 1c). Groups of participants were either incentivized on the individual or group level (between-subjects factor). In the “Individual Incentives” condition, participants’ reward payment depended solely on their own amount of coins collected. In the “Group Incentives” condition, participants were rewarded based on the average number of coins collected across all four group members. As a second (within-subjects) factor, we manipulated the resource distribution: The same number of coin resources was either concentrated in few but rich patches (“Concentrated” condition; 5 patches with 48 coins each) or distributed among many but poor patches (“Distributed” condition; 15 patches with 16 coins each). Participants experienced each resource distribution twice and all possible permutations of presentation order were realized for both incentive conditions. The resource distribution for each round was announced prior to the start of each round and was also indicated by the

color of the walls enclosing the arena. Participants in the individual foraging condition searched for coins on their own with the same resource distributions and were paid depending on the number of coins collected.

Data

At a sampling interval of 25Hz, we recorded participants’ (1) X- and Y-coordinates, (2) orientation vector, (3) velocity, (4) coin count and (5) whether they were extracting or not. From this raw data, we constructed movement trajectories of all players and computed the full visual social information available at each point in time through basic triangulation (video S3; see GitHub repository for complete data-processing scripts: <https://github.com/DominikDeffner/VirtualCollectiveForaging>). Moreover, we recorded (1) when a player arrived at a patch, (2) when a player extracted a coin, (3) when a patch was depleted, and (4) when and where a new patch was generated. For each event involving a player, we recorded the time stamp and ID of the player.

Behavioral analyses

Temporal dynamics of success

To quantify how participants’ performance changes over time, we used a multilevel model with Bernoulli likelihood to predict whether players are currently exploiting a patch on a one-second resolution. In addition to intercepts for each experimental condition and individual- and group-specific offsets, we used time (minute in round) as an ordered categorical (or monotonic) predictor, which also varied by condition. Instead of imposing a particular functional form (e.g., a line), this approach only assumes that performance changes monotonically over time (i.e. either constantly increases or decreases) and lets the model estimate the size of the steps in which success probabilities change [15, 64]:

$$P(E)_{ij}^{\tilde{t}} = \text{logit}^{-1}(\alpha_{ij} + \beta_{ij}^{\text{MAX}} \sum_{m=0}^{\tilde{t}-1} \delta_{ij}^m). \quad (2)$$

The probability that players are exploiting in a specific minute of a round, indicated by \tilde{t} , is composed of the intercept for each incentive condition i and environment j and the total effect of experimental time multiplied by a sum of δ -parameters which represent the additional effect of each increment in time (all δ s together sum to 1).

Scrounging analysis

To infer behavioral scrounging rates, we computed conditional probabilities for players to join a patch where they observed at least one exploiting group member. We first computed at which patches players observed an exploiting group member and then modeled the proportion of those patches that players actually joined using a binomial likelihood function. In addition to condition-specific intercepts, we implemented individual- and group-level random effects. This also allowed us to use estimated individual-level scrounging rates (compared to other group members) to predict success in both environments within the same model propagating the full range of uncertainty (Fig. 2d; top).

Social Hidden Markov Decision Model

We used a computational approach to study how different social and asocial cues impact participants' decisions to use social information and switch between behavioral states across the different conditions. Inspired by tools and concepts from animal movement ecology [27, 28, 65], we developed a novel Social Hidden Markov Decision Model. A Hidden Markov model is a doubly-stochastic time-series model with an observation process and an underlying state process (Fig. 1d). It resembles a finite mixture model with several outcome variables where the identity of the underlying distributions is controlled by a Markov chain [66]. The model uses time series of "state-dependent variables" (on a one-second resolution) to probabilistically assign each time point per participant to one of a fixed number of latent behavioral states. Participants can be in three different states: individual exploration, social relocation and exploitation [67]. Since exploitation is observed, our only hidden states are individual exploration and social relocation and the model estimates parameters of the distributions that characterize both states. Additionally, our Social Hidden Markov Decision Model simultaneously infers the transition probabilities between both latent behavioral states and we included time-dependent (social and asocial) "state predictors" that influence such transitions.

State-dependent Variables

We used three state-dependent variables to infer the latent states from the data: (1) participants' turning angles (change in movement direction in radians between successive time points; social relocation is expected to be characterized by directed movement, i.e., small turning angles), (2) the (smallest) change in distance to visible exploiting player(s) (social relocation marked by large reduction in distance to observed exploiting players) and (3) the (smallest) relative bearing (angle between orientation vector and vector connecting focal player to each other player; social relocation marked by consistent orientation towards other player, i.e., small relative bearing). Figure S7, top three rows, illustrates the state-dependent variables for one exemplary time series with orange bars representing periods identified by the model as social information use through the Viterbi algorithm [68, 69]. To model the turning angles, we used the von Mises distribution which is commonly used in directional statistics for continuous circular data. It is a (more tractable) close approximation of the Wrapped normal distribution [70]. For change in distance and relative bearings, we used normal and log-normal likelihoods, respectively.

State Predictors

To quantify how experimental conditions and situational factors modify each participant's probability to stop exploring independently and switch to social relocation at each time point t , we used four state predictors (Fig. S7, bottom four rows): (1) a binary visibility indicator ($V = 1$ if any exploiting player is currently in field of view, $V = 0$ otherwise), (2) the (z-standardized) distance to the closest *visible* exploiting player D , (3) the number of other players extracting at the closest *visible* patch N (coded such that $N = 0$ represents the default where only one player is exploiting) and (4) the (z-standardized) time since the last coin extraction T . All state predictors were estimated for each incentive condition

i and environment j (Eq. 1). Note that D_t and N_t are multiplied by V_t in Eq. 1 to "switch on" the effects of distance and player number only for times when participants actually observed (an) exploiting player(s), i.e., when $V_t = 1$. All predictor weights were estimated in a fully hierarchical Bayesian framework with random-effect terms accounting for the covariance of decision weights among both individuals and groups while also allowing those covariances to differ among experimental conditions (omitted from Eq. 1 for the sake of readability).

Time-varying state predictors

Moreover, we augmented these multilevel models by estimating time-varying parameters through ordered categorical (monotonic) effects and describe how social decision-making dynamics unfold over time. As one example (other state predictors are constructed equivalently), the effect of patch distance on the probability to switch to social relocation in a specific minute of a round \tilde{t} is composed of the total effect of time times the sum of δ -parameters which represent the additional effect of each increment in time:

$$\beta_{D_{ij}}^{\tilde{t}} = \beta_{D_{ij}^{\text{MAX}}} \sum_{m=0}^{\tilde{t}-1} \delta_{D_{ij}^m}. \quad (3)$$

Note we only included individual- and group-specific offsets for the average effect of each state predictor over time.

Forward and Viterbi algorithms

To efficiently compute the (log) marginal likelihood, i.e., the joint distribution of each data sequence summing over all possible state sequences, we used the *forward algorithm*, which calculates this likelihood recursively [see 27, 65, 66, 68, for more technical introductions]. After model fitting, we used the dynamic-programming *Viterbi algorithm* to obtain the most likely state sequence given the observations and estimated parameters [27, 66, 68]. This reconstruction of the underlying state sequence helps visualizing the results of the fitted models and ensuring that the state-dependent distributions can be connected to psychologically meaningful processes. We only explicitly modeled times at which players potentially could use social information, i.e., times when they were allowed to move and at least one group member was currently collecting coins (white segments in Fig. S7). This means we omitted all times (1) when players themselves were exploiting a patch (dark grey segments in Fig. S7) and (2) when no group member was exploiting (light grey segments in Fig. S7), because in both cases we know the state of a player. To ensure a proper latent state sequence, we set a player's state to individual exploration after both types of omissions.

Collective Visual-Spatial Dynamics Model

Lastly, we investigated how the visual-spatial organization of groups affected collective success across different timescales and how these dynamics differed among incentive conditions and environments. Specifically, we used a time-lagged Gaussian-process regression model with binomial likelihood to estimate how spatial and visual organization at different times in the past $t - \tau$ (in steps of 5 seconds for up to three minutes, i.e., $t - 5s, t - 10s, \dots, t - 180s$, as well as for each

second for up to half a minute, i.e., $t-1s, t-2s, \dots, t-30s$) predicted collective success (proportion of players exploiting) at time t . Gaussian processes extend the multilevel approach to continuous categories and estimate a unique parameter value for each category, while still regarding time as a continuous dimension in which similar time lags are expected to generate similar estimates [64]. The regression weight for a given time lag $t-\tau$ (for incentive condition i and environment j) is composed of the average effect and a lag-specific offset for each experimental condition:

$$\beta_{ij}^{t-\tau} = \bar{\beta}_{ij} + d_{ij}^{\tau}. \quad (4)$$

The lag-specific offsets follow a multivariate Gaussian distribution, separately for experimental conditions:

$$\begin{pmatrix} d_{ij}^1 \\ d_{ij}^2 \\ \dots \\ d_{ij}^{max} \end{pmatrix} \sim N \left(\begin{pmatrix} 0 \\ 0 \\ \dots \\ 0 \end{pmatrix}, K_{ij} \right). \quad (5)$$

The vector of means is all zeros, so the average effect remains unchanged, and K_{ij} is the covariance matrix among time lags. We estimated the parameters of a Radial basis function (or “squared-exponential”) kernel that expresses how the covariance between different lags changes as the distance between them increases:

$$K_{ij}^{\tau_x \tau_y} = \eta_{ij} \exp\left(-\rho_{ij} \frac{(\tau_y - \tau_x)^2}{\tau_{max}^2}\right). \quad (6)$$

The covariance between time lags τ_x and τ_y equals the maximum covariance η_{ij} , which is reduced at rate ρ_{ij} by the relative squared distance between τ_x and τ_y .

Model fitting

All models were fitted using Stan as a Hamiltonian Monte Carlo engine for Bayesian inference [71], implemented in R v.4.0.3 through cmdstanr version 0.3.0.9 [72]. We used within-chain parallelization with `reduce_sum` to substantially reduce model run times through parallel evaluation of the likelihood. To reduce the risk of overfitting the data, we generally used weakly informative priors for all parameters. For state-dependent distributions in the Social Hidden Markov Decision Model, we used informative priors to incorporate knowledge about the nature of both states which also helps avoid label-switching, a common issue in all mixture models [27, 68]. To optimize convergence, we implemented the non-centered version of random effects using a Cholesky decomposition of the correlation matrix [64] with LKJ priors for correlations matrices [73]. Visual inspection of traceplots and rank histograms [74] suggested good model convergence and no other pathological chain behaviors, with convergence confirmed by the Gelman-Rubin criterion [75] $\hat{R} \leq 1.01$. All inferences are based on several hundred effective samples from the posterior [76]. See GitHub repository for full model code and analysis scripts: <https://github.com/DominikDeffner/VirtualCollectiveForaging>.

Acknowledgements

We thank Jann Wäscher for recruiting participants, Philip Jakob for technical support, and Pietro Nickl for helping with

Figure 1. This research has been supported by the Deutsche Forschungsgemeinschaft (DFG, German Research Foundation) under Germany’s Excellence Strategy – EXC 2002/1 "Science of Intelligence" – project number 390523135. CMW is supported by the German Federal Ministry of Education and Research (BMBF): Tübingen AI Center, FKZ: 01IS18039A and funded by the Deutsche Forschungsgemeinschaft (DFG, German Research Foundation) under Germany’s Excellence Strategy–EXC2064/1–390727645. The funders had no role in study design, data collection and analysis, decision to publish, or preparation of the manuscript.

Data Accessibility

All relevant data and code are stored on GitHub: <https://github.com/DominikDeffner/VirtualCollectiveForaging>.

Author contributions statement

DD and RHJMK conceived the experiment, with feedback from DM, BK, CMW, and PR. DD, BK, and RHJMK performed the experiments. DD processed the data, analyzed the results and prepared the figures, with input from AS, CMW and RHJMK. DD wrote the first draft and all authors reviewed the manuscript.

Competing interests

The authors declare no competing interests.

References

1. Galesic M, et al., 2023 Beyond collective intelligence: Collective adaptation. *Journal of the Royal Society Interface* **20**, 20220736
2. Tump AN, Deffner D, Pleskac T, Romanczuk P, Kurvers R, (in press) A cognitive computational approach to social and collective decision-making. *Perspectives on Psychological Science*
3. Krause J, Romanczuk P, Cracco E, Arlidge W, Nassauer A, Brass M, 2021 Collective rule-breaking. *Trends in Cognitive Sciences* **25**, 1082–1095
4. Wu CM, Dale R, Hawkins RD, submitted Group coordination catalyzes individual and cultural intelligence. *PsyArXiv*
5. Giraldeau LA, Valone TJ, Templeton JJ, 2002 Potential disadvantages of using socially acquired information. *Philosophical Transactions of the Royal Society of London. Series B: Biological Sciences* **357**, 1559–1566
6. Rogers AR, 1988 Does biology constrain culture? *American Anthropologist* **90**, 819–831
7. Kendal RL, Boogert NJ, Rendell L, Laland KN, Webster M, Jones PL, 2018 Social learning strategies: Bridge-building between fields. *Trends in cognitive sciences* **22**, 651–665
8. Laland KN, 2004 Social learning strategies. *Animal Learning & Behavior* **32**, 4–14
9. Aoki K, Feldman MW, 2014 Evolution of learning strategies in temporally and spatially variable environments: a review of theory. *Theoretical population biology* **91**, 3–19
10. Giraldeau LA, Caraco T, 2000 *Social foraging theory*. Princeton University Press
11. Mesoudi A, O’Brien MJ, 2008 The cultural transmission of great basin projectile-point technology i: an experimental simulation. *American Antiquity* **73**, 3–28
12. Mesoudi A, 2008 An experimental simulation of the “copy-successful-individuals” cultural learning strategy: Adaptive landscapes, producer-scrounger dynamics, and informational access costs. *Evolution and Human Behavior* **29**, 350–363

- 920 13. Miu E, Gulley N, Laland KN, Rendell L, 2020 Flexible learning, 995
rather than inveterate innovation or copying, drives cumulative knowledge gain. *Science advances* **6**, eaaz0286
- 925 14. McElreath R, Lubell M, Richerson PJ, Waring TM, Baum W, Edsten E, Efferson C, Paciotti B, 2005 Applying evolutionary models to the laboratory study of social learning. *Evolution and Human Behavior* **26**, 483–508
- 930 15. Deffner D, Kleino V, McElreath R, 2020 Dynamic social learning in temporally and spatially variable environments. *Royal Society open science* **7**, 200734
- 935 16. Toyokawa W, Whalen A, Laland KN, 2019 Social learning strategies regulate the wisdom and madness of interactive crowds. *Nature Human Behaviour* **3**, 183–193
- 940 17. Toyokawa W, Gaissmaier W, 2022 Conformist social learning leads to self-organised prevention against adverse bias in risky decision making. *Elife* **11**, e75308
- 945 18. Witt A, Toyokawa W, Gaissmaier W, Lala K, Wu CM, 2023 Social learning with a grain of salt. *PsyArXiv*
- 950 19. Strandburg-Peshkin A, et al., 2013 Visual sensory networks and effective information transfer in animal groups. *Current Biology* **23**, R709–R711
- 955 20. Wu CM, Deffner D, Kahl B, Meder B, Ho MH, Kurvers RH, 2023 Visual-spatial dynamics drive adaptive social learning in immersive environments. *bioRxiv*
- 960 21. Bastien R, Romanczuk P, 2020 A model of collective behavior based purely on vision. *Science advances* **6**, eaay0792
- 965 22. Vickery WL, Giraldeau LA, Templeton JJ, Kramer DL, Chapman CA, 1991 Producers, scroungers, and group foraging. *The american naturalist* **137**, 847–863
- 970 23. Barta Z, Flynn R, Giraldeau LA, 1997 Geometry for a selfish foraging group: a genetic algorithm approach. *Proceedings of the Royal Society of London. Series B: Biological Sciences* **264**, 1233–1238
- 975 24. Beauchamp G, 2008 A spatial model of producing and scrounging. *Animal Behaviour* **76**, 1935–1942
- 980 25. Kurvers RH, Hamblin S, Giraldeau LA, 2012 The effect of exploration on the use of producer-scrounger tactics. *PloS one* **7**, e49400
- 985 26. Deffner D, McElreath R, 2022 When does selection favor learning from the old? social learning in age-structured populations. *PloS one* **17**, e0267204
- 990 27. Leos-Barajas V, Michelot T, 2018 An introduction to animal movement modeling with hidden markov models using stan for bayesian inference. *arXiv preprint arXiv:1806.10639*
28. Auger-Méthé M, et al., 2021 A guide to state-space modeling of ecological time series. *Ecological Monographs* **91**, e01470
29. Kandler A, Powell A, 2018 Generative inference for cultural evolution. *Philosophical Transactions of the Royal Society B: Biological Sciences* **373**, 20170056
30. Rosati AG, 2017 Foraging cognition: reviving the ecological intelligence hypothesis. *Trends in cognitive sciences* **21**, 691–702
31. Kaplan H, Hill K, Lancaster J, Hurtado AM, 2000 A theory of human life history evolution: Diet, intelligence, and longevity. *Evolutionary Anthropology: Issues, News, and Reviews: Issues, News, and Reviews* **9**, 156–185
32. Henrich J, McElreath R, 2003 The evolution of cultural evolution. *Evolutionary Anthropology: Issues, News, and Reviews: Issues, News, and Reviews* **12**, 123–135
33. Henrich J, 2017 *The secret of our success: How culture is driving human evolution, domesticating our species, and making us smarter*. Princeton University Press
34. Schuppli C, Isler K, van Schaik CP, 2012 How to explain the unusually late age at skill competence among humans. *Journal of human evolution* **63**, 843–850
35. González-Forero M, Gardner A, 2018 Inference of ecological and social drivers of human brain-size evolution. *Nature* **557**, 554–557
36. Monk CT, Barbier M, Romanczuk P, Watson JR, Alós J, Nakayama S, Rubenstein DI, Levin SA, Arlinghaus R, 2018 How ecology shapes exploitation: a framework to predict the behavioural response of human and animal foragers along exploration-exploitation trade-offs. *Ecology letters* **21**, 779–793
37. Garg K, Kello C, Smaldino P, 2022 Individual exploration and selective social learning: Balancing exploration-exploitation trade-offs in collective foraging. *Journal of The Royal Society Interface* **19**
38. Barbier M, Watson JR, 2016 The spatial dynamics of predators and the benefits and costs of sharing information. *PLoS computational biology* **12**, e1005147
39. Torney CJ, Berdahl A, Couzin ID, 2011 Signalling and the evolution of cooperative foraging in dynamic environments. *PLoS computational biology* **7**, e1002194
40. Berdahl A, Torney CJ, Ioannou CC, Faria JJ, Couzin ID, 2013 Emergent sensing of complex environments by mobile animal groups. *Science* **339**, 574–576
41. Hawkins RD, Berdahl AM, Pentland A, Tenenbaum JB, Goodman ND, Krafft P, et al., 2022 Flexible social inference facilitates targeted social learning when rewards are not observable. *arXiv preprint arXiv:2212.00869*
42. Adjerid I, Kelley K, 2018 Big data in psychology: A framework for research advancement. *American Psychologist* **73**, 899
43. Couzin ID, Heins C, 2022 Emerging technologies for behavioral research in changing environments. *Trends in Ecology & Evolution*
44. Garg K, Kello CT, 2021 Efficient lévy walks in virtual human foraging. *Scientific reports* **11**, 1–12
45. Spiers HJ, Coutrot A, Hornberger M, 2023 Explaining worldwide variation in navigation ability from millions of people: citizen science project sea hero quest. *Topics in cognitive science* **15**, 120–138
46. Moussaïd M, Perozo N, Garnier S, Helbing D, Theraulaz G, 2010 The walking behaviour of pedestrian social groups and its impact on crowd dynamics. *PloS one* **5**, e10047
47. Moussaïd M, Helbing D, Theraulaz G, 2011 How simple rules determine pedestrian behavior and crowd disasters. *Proceedings of the National Academy of Sciences* **108**, 6884–6888
48. Keshri S, Oh Mh, Zhang S, Iyengar G, 2019 Automatic event detection in basketball using hmm with energy based defensive assignment. *Journal of Quantitative Analysis in Sports* **15**, 141–153
49. Ali I, 2019. Tagging basketball events with hmm in stan. <https://mc-stan.org/users/documentation/case-studies/bball-hmm.html>. Accessed: 2023-05-03
50. Ötting M, Langrock R, Deutscher C, Leos-Barajas V, 2020 The hot hand in professional darts. *Journal of the Royal Statistical Society Series A: Statistics in Society* **183**, 565–580
51. Strandburg-Peshkin A, Farine DR, Couzin ID, Crofoot MC, 2015 Shared decision-making drives collective movement in wild baboons. *Science* **348**, 1358–1361
52. Strandburg-Peshkin A, Papageorgiou D, Crofoot MC, Farine DR, 2018 Inferring influence and leadership in moving animal groups. *Philosophical Transactions of the Royal Society B: Biological Sciences* **373**, 20170006
53. Pacheco-Cobos L, Winterhalder B, Cuatianquiz-Lima C, Rosetti MF, Hudson R, Ross CT, 2019 Nahua mushroom gatherers use area-restricted search strategies that conform to marginal value theorem predictions. *Proceedings of the National Academy of Sciences* **116**, 10339–10347
54. Wood BM, et al., 2021 Gendered movement ecology and landscape use in hadza hunter-gatherers. *Nature Human Behaviour* **5**, 436–446
55. Ford JD, Tillear SE, Berrang-Ford L, Araos M, Biesbroek R, Lesnikowski AC, MacDonald GK, Hsu A, Chen C, Bizikova L, 2016 Big data has big potential for applications to climate change adaptation. *Proceedings of the National Academy of Sciences* **113**, 10729–10732
56. Szocska M, et al., 2021 Countrywide population movement monitoring using mobile devices generated (big) data during the covid-19 crisis. *Scientific Reports* **11**, 5943
57. Kays R, Crofoot MC, Jetz W, Wikelski M, 2015 Terrestrial animal tracking as an eye on life and planet. *Science* **348**, aaa2478
58. Kays R, et al., 2022 The movebank system for studying global animal movement and demography. *Methods in Ecology and Evolution* **13**, 419–431

- 1065 59. Nathan R, *et al.*, 2022 Big-data approaches lead to an increased understanding of the ecology of animal movement. *Science* **375**, eabg1780
60. Henrich J, Heine SJ, Norenzayan A, 2010 Most people are not weird. *Nature* **466**, 29–29
- 1070 61. Deffner D, Rohrer JM, McElreath R, 2022 A causal framework for cross-cultural generalizability. *Advances in Methods and Practices in Psychological Science* **5**, 25152459221106366
62. Unity Technologies, 2021. Unity user manual. <https://docs.unity3d.com/2020.3/Documentation/Manual/index.html>. Accessed: 2023-05-03
- 1075 63. Unity Technologies, 2021. Unity 2020.3.21. <https://unity.com/releases/editor/whats-new/2020.3.21>. Accessed: 2023-05-03
64. McElreath R, 2020 *Statistical rethinking: A Bayesian course with examples in R and Stan*. CRC press
- 1080 65. McClintock BT, Langrock R, Gimenez O, Cam E, Borchers DL, Glennie R, Patterson TA, 2020 Uncovering ecological state dynamics with hidden markov models. *Ecology letters* **23**, 1878–1903
66. Bishop CM, Nasrabadi NM, 2006 *Pattern recognition and machine learning*, vol. 4. Springer
- 1085 67. Bartumeus F, Campos D, Ryu WS, Lloret-Cabot R, Méndez V, Catalán J, 2016 Foraging success under uncertainty: search tradeoffs and optimal space use. *Ecology letters* **19**, 1299–1313
68. Zucchini W, MacDonald IL, Langrock R, 2017 *Hidden Markov models for time series: an introduction using R*. CRC press
- 1090 69. Forney GD, 1973 The viterbi algorithm. *Proceedings of the IEEE* **61**, 268–278
70. Pewsey A, Neuhauser M, Ruxton GD, 2013 *Circular statistics in R*. Oxford University Press
- 1095 71. Carpenter B, Gelman A, Hoffman MD, Lee D, Goodrich B, Betancourt M, Brubaker M, Guo J, Li P, Riddell A, 2017 Stan: A probabilistic programming language. *Journal of statistical software* **76**
72. Gabry J, Češnovar R, 2020 cmdstanr: R interface to 'cmdstan'. See mc-stan.org/cmdstanr/reference/cmdstanr-package.html
- 1100 73. Lewandowski D, Kurowicka D, Joe H, 2009 Generating random correlation matrices based on vines and extended onion method. *Journal of multivariate analysis* **100**, 1989–2001
74. Vehtari A, Gelman A, Simpson D, Carpenter B, Bürkner PC, 2019 Rank-normalization, folding, and localization: An improved \hat{R} for assessing convergence of mcmc. *arXiv preprint arXiv:1903.08008*
- 1105 75. Gelman A, Rubin DB, *et al.*, 1992 Inference from iterative simulation using multiple sequences. *Statistical Science* **7**, 457–472
- 1110 76. Gelman A, Carlin JB, Stern HS, Dunson DB, Vehtari A, Rubin DB, 2013 *Bayesian data analysis*. Chapman and Hall/CRC

Electronic Supplementary Material for

Collective incentives reduce over-exploitation of social information in unconstrained human groups

Dominik Deffner^{1,2*}, David Mezey^{2,3}, Benjamin Kahl¹, Alexander Schakowski¹, Paweł Romanczuk^{2,3}, Charley Wu^{1,4,5} & Ralf Kurvers^{1,2}

¹Center for Adaptive Rationality, Max Planck Institute for Human Development, Berlin, Germany

²Science of Intelligence Excellence Cluster, Technical University Berlin, Berlin, Germany

³Institute for Theoretical Biology, Humboldt University Berlin, Berlin, Germany

⁴University of Tübingen, Tübingen, Germany

⁵Max Planck Institute for Biological Cybernetics, Tübingen, Germany

*deffner@mpib-berlin.mpg.de

A. Supplementary Videos

Video S1. Example of participants' first-person field of view during the experiment.

Video S2. Example video of in-game tutorial.

Video S3. Illustration of the visual field reconstruction.

B. Supplementary Figures

Figure S1. Exploitation probabilities over time.

Figure S2. Additional behavioral results.

Figure S3. Behavioral results at the group level.

Figure S4. Movement metrics and independent discoveries.

Figure S5. Behavioral results for individual foragers.

Figure S6. Movement metrics and independent discoveries for individual foragers.

Figure S7. Exemplary time-series data for the Social Hidden Markov Decision model.

Figure S8. State-dependent distributions from the Social Hidden Markov Decision model.

Figure S9. Influence of average decision weights on collective foraging success.

Figure S10. Temporal dynamics in state predictors using linear trends.

Figure S11. Collective visual-spatial dynamics for up to 3-minute time lags.

C. Preregistration document (OSF link: <https://osf.io/5r736/>)

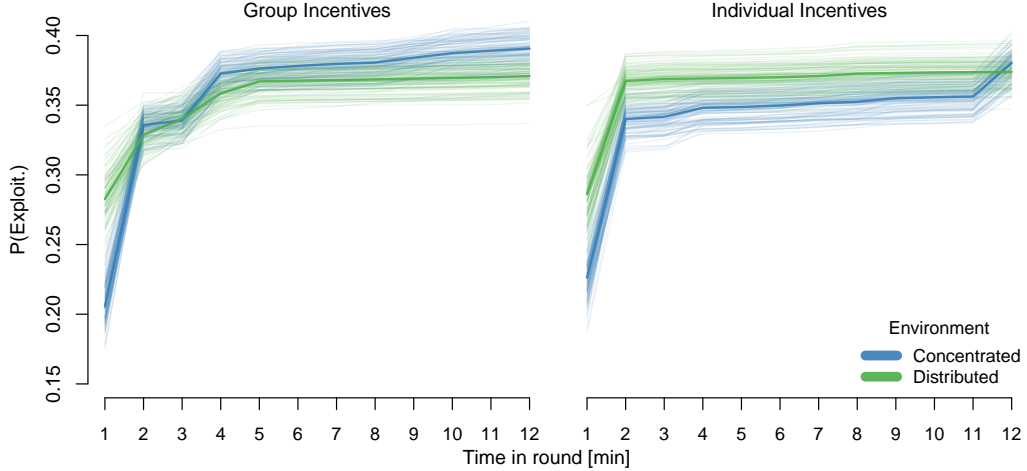


Figure S1. Exploitation probabilities over time 100 random draws from the posterior distribution (transparent lines) as well as posterior means (solid lines) for the probability that players are successful (i.e., exploiting a patch) over time per incentive condition and environment. Results come from multilevel logistic regression with time in round as an ordered categorical (monotonic) predictor.

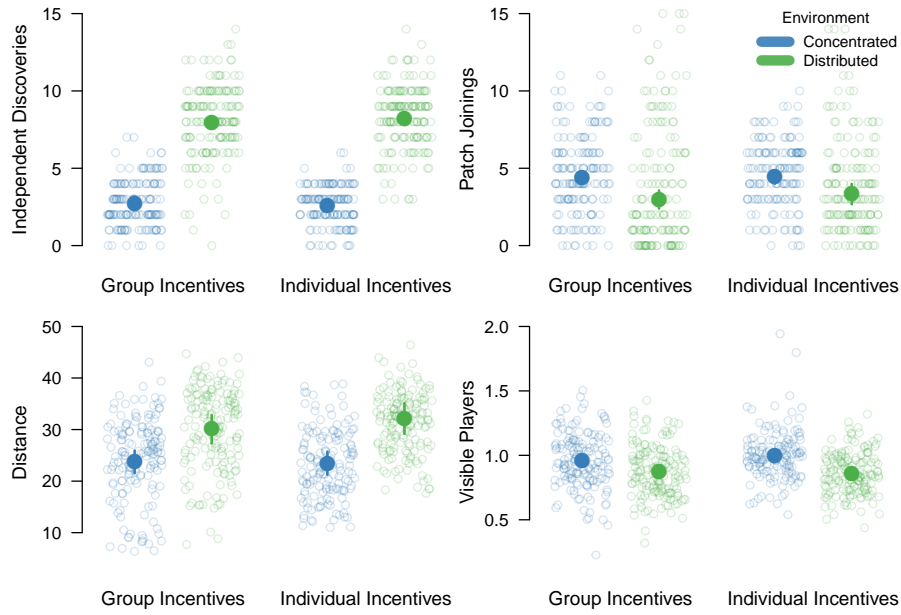


Figure S2. Additional behavioral results. Number of independent patch discoveries and patch joinings, as well as distance (average distance to the other three players for times when focal player was not exploiting) and visibility (average number of players in field of view when focal player was not exploiting). Each circle represents data from one round per participant, larger filled dots represent posterior estimates (as well as 90% HPDIs) from Bayesian multilevel models.

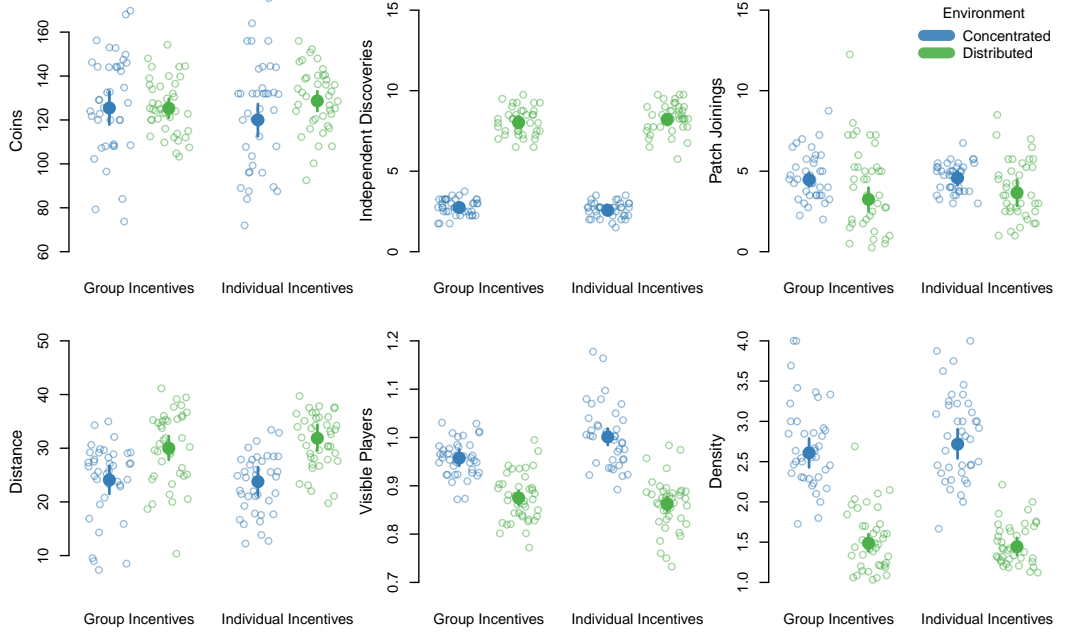


Figure S3. Behavioral results at the group level. Average number of coins collected, independent patch discoveries, patch joinings, distance (average distance to the other three players for times when focal player was not exploiting), visibility (average number of players in field of view when focal player was not exploiting), and density (average number of foragers exploiting at discovered patches) per environment and incentive condition. Each circle represents data from one round for each group of participants. Larger filled dots represent posterior estimates (as well as 90% HPDIs) from Bayesian multilevel models accounting for group-level variability.

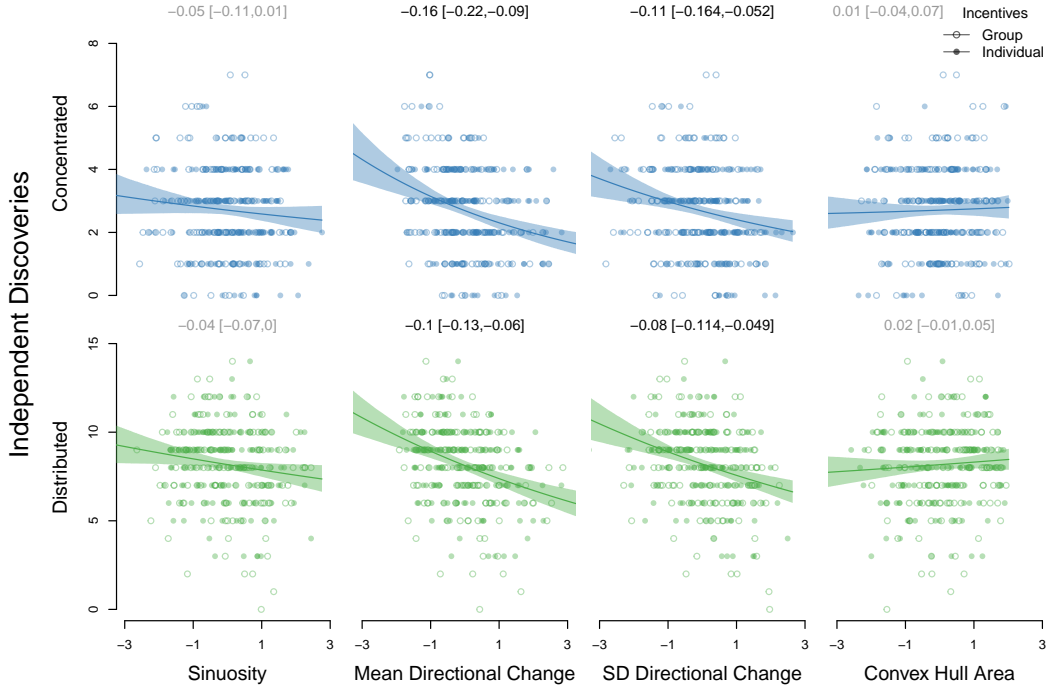


Figure S4. Movement metrics and independent discoveries. Number of patches independently discovered in each round by individuals in concentrated and distributed environments as a function of different metrics describing each movement trajectory (using the *trajr* r package by McLean and Skowron Volponi, 2018): (1) Sinuosity index (Benhamou, 2004), (2) the mean of directional changes (measure of nonlinearity), (3) the standard deviation of directional changes (measure of irregularity) (Kitamura and Imafuku, 2015) as well as (4) the convex hull area (area of smallest convex set containing all locations a participant visited). Open circles represent participants in the “Group Incentives” condition, filled circles represent participants in the “Individual Incentives” condition. Lines and uncertainty intervals show the effect of each variable (reported above, transparent text if 90% HPDI overlaps 0) from Bayesian Poisson regressions accounting for baseline differences between conditions. All predictors were z-standardized before the analysis.

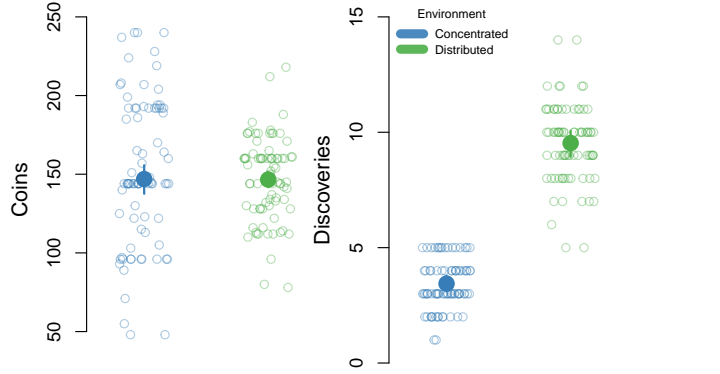


Figure S5. Behavioral results for individual foragers. Number of coins collected and independent patch discoveries for different environments. Each transparent circle represents data from one round for one participant. Larger filled dots represent posterior estimates (as well as 90% HPDIs) from Bayesian multilevel models.

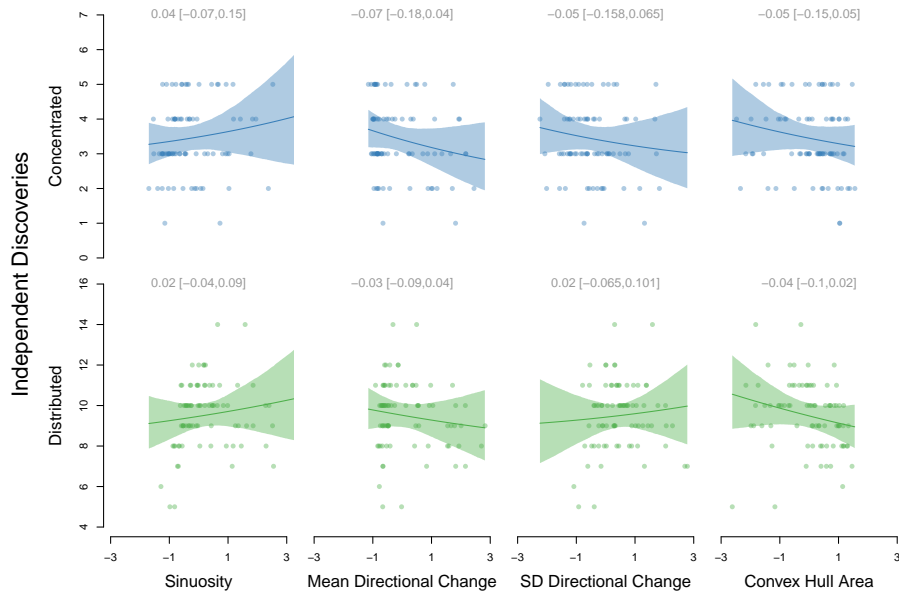


Figure S6. Movement metrics and independent discoveries for individual foragers. Number of patches discovered in each round by individuals in concentrated and distributed environments as a function of different metrics describing each movement trajectory (using the trajr r package by McLean and Skowron Volponi, 2018): (1) Sinuosity index (Benhamou, 2004), (2) the mean of directional changes (measure of nonlinearity), (3) the standard deviation of directional changes (measure of irregularity) (Kitamura and Imafuku, 2015) as well as (4) the convex hull area (area of smallest convex set containing all locations a participant visited). Lines and uncertainty intervals show the effect of each variable (reported above, transparent text if 90% HPDI overlaps 0) from Bayesian Poisson regressions. All predictors were z-standardized before the analysis.

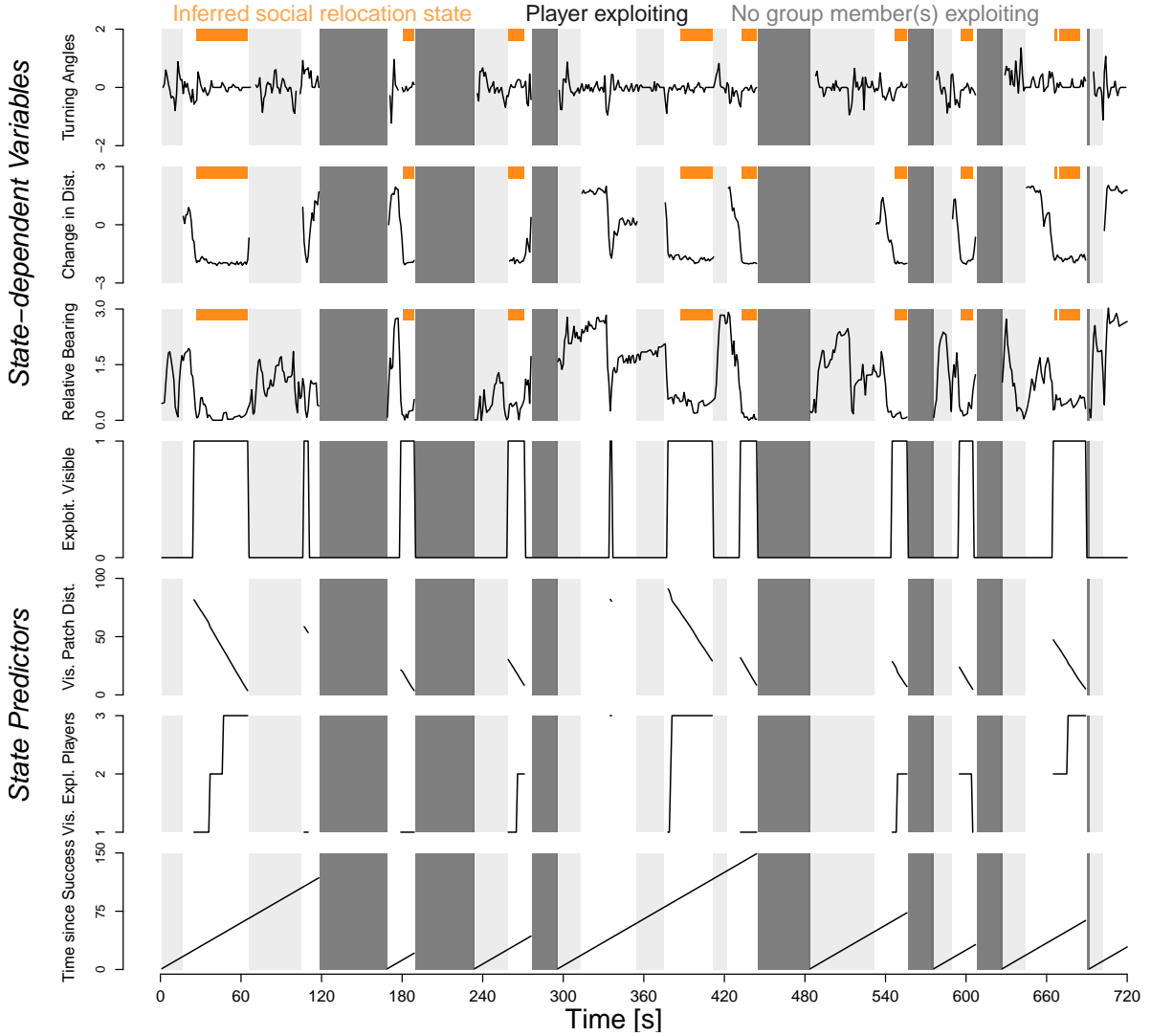


Figure S7. Exemplary time-series data for the Social Hidden Markov Decision Model. *State-dependent Variables* used to identify latent behavioral states include (1) turning angles (change in movement direction between successive time points; in radians), (2) (smallest) change in distance to exploiting player(s) across time points and (3) relative bearing (smallest angle between orientation vector of player and locations of other players). *State Predictors* used to model latent transition probabilities between behavioral states include (1) a binary visibility indicator V (“Is any exploiting player in field of view?”), (2) the distance to the closest visible exploited patch D , (3) the number of other players extracting at the closest visible patch N as well as (4) the time since the last success (coin extraction) T . Trajectories show one data point per second, the same temporal resolution as used in the computational model. Exploitation times when a player was collecting coins at a patch are marked by dark grey areas. Lighter grey areas represent periods when no other player was collecting coins. In both cases, we know the state of the focal player (exploitation and individual exploration, respectively), so we only explicitly model periods when players potentially could use social information. Orange bars represent time periods identified by the Viterbi algorithm as social relocation.

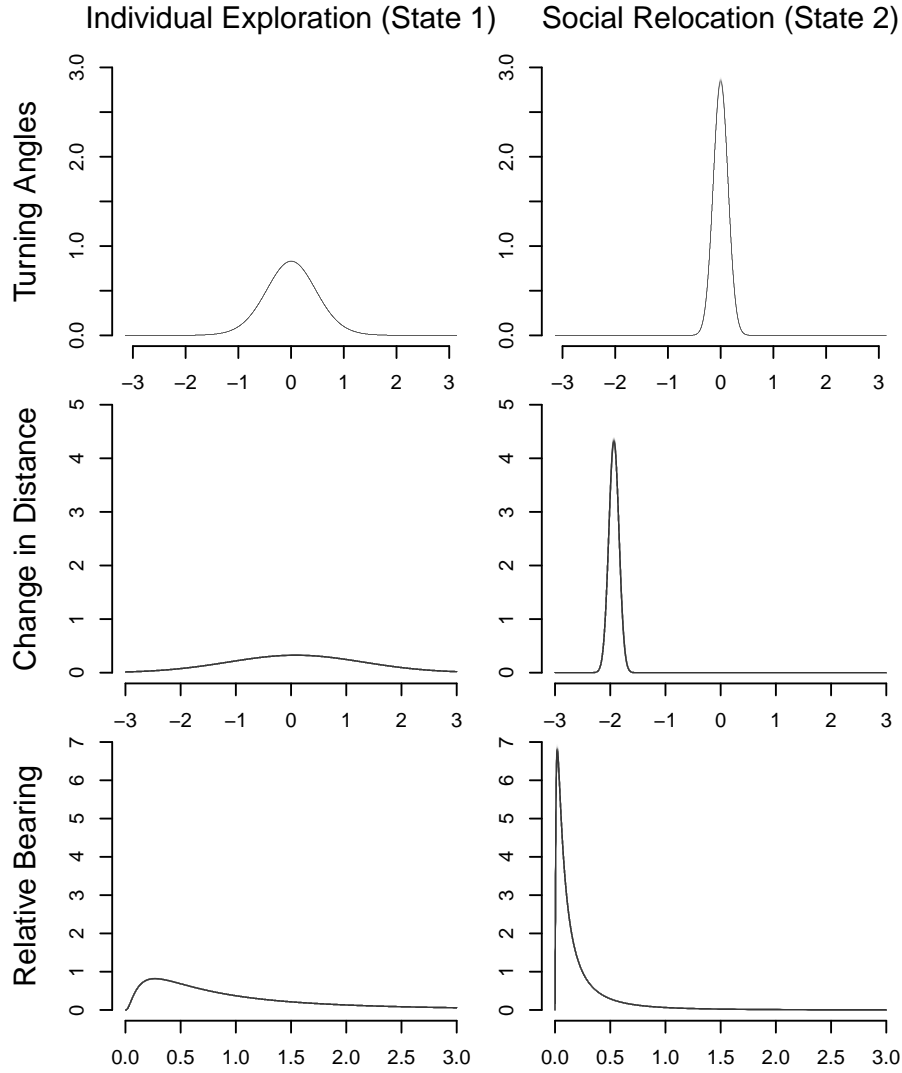


Figure S8. State-dependent distributions from the Social Hidden Markov Decision Model. Von Mises distributions for turning angles (top), Gaussian distributions for change in distance to exploiting players (middle) and lognormal distributions for relative bearing (bottom) based on 100 random draws from the posterior for state 1 (“Individual Exploration”) and state 2 (“Social Relocation”). Lines look almost identical due to the very narrow posterior parameter estimates defining those distributions, which are derived from almost 150k observations. Note the greater variability in behavior during individual exploration results in substantially wider distributions for all three variables .

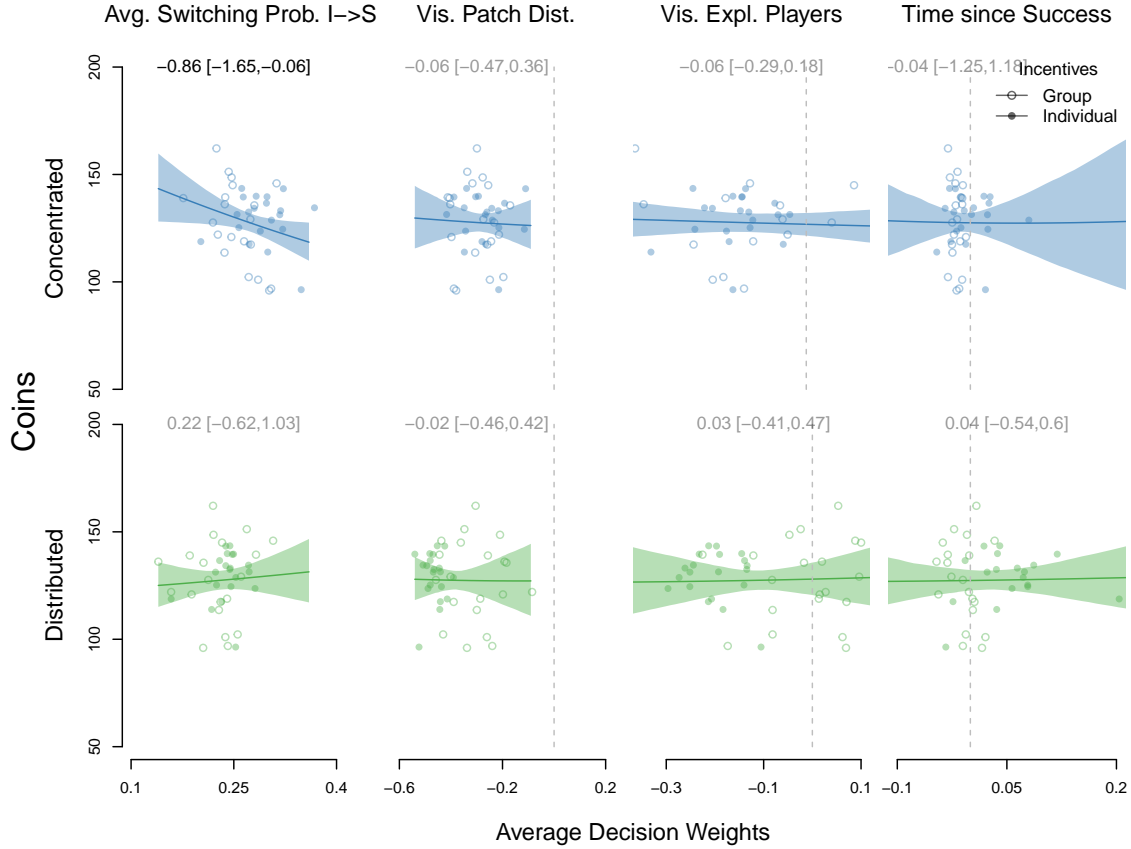


Figure S9. Influence of average decision weights on collective foraging success. Success (average number of coins collected by each group) in concentrated and distributed environments as a function of average individual-level weights derived from the Social Hidden Markov Decision Model. Open circles represent groups in the “Group Incentives” condition, filled circles represent groups in the “Individual Incentives” condition. Lines and uncertainty intervals show the effect of each decision weight (reported above, transparent text if 90% HPDI overlaps 0) from Bayesian log-normal regression models accounting for baseline success differences between conditions.

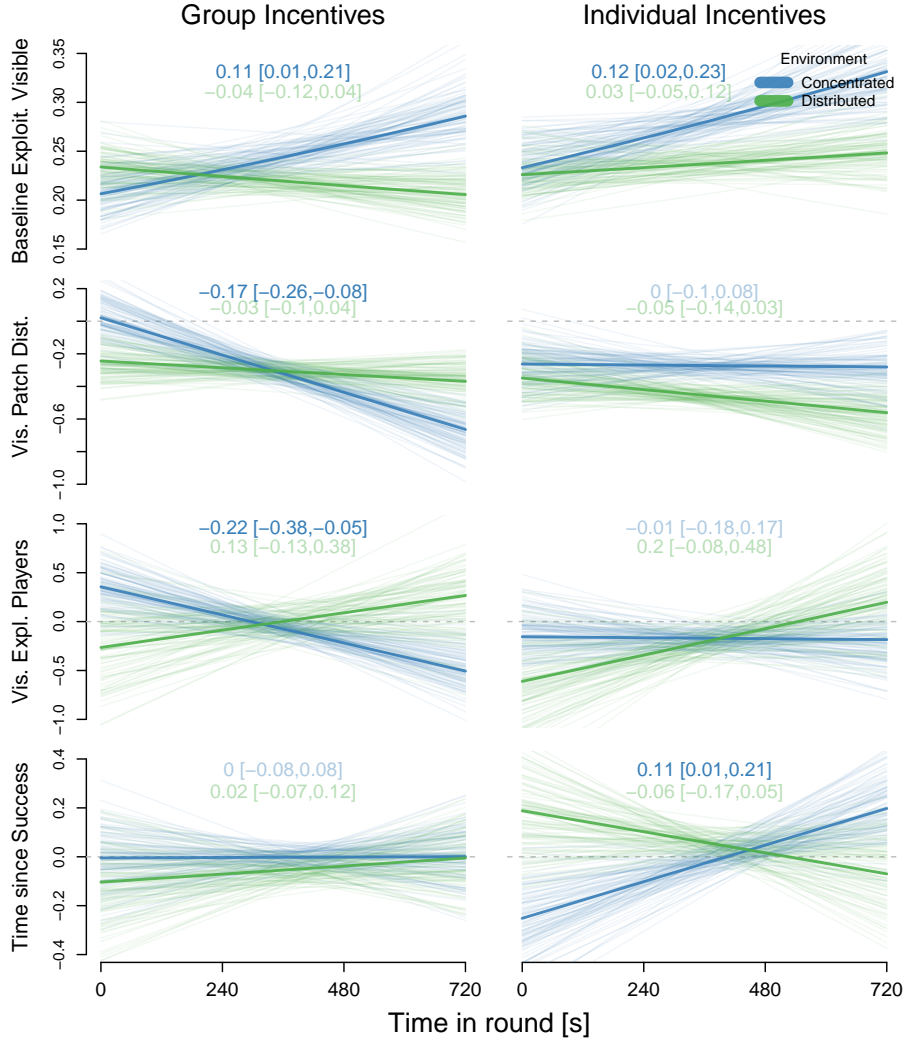


Figure S10. Computational modelling results: Temporal dynamics in state predictors using linear trends. 100 random draws from the posterior distribution (transparent lines) as well as posterior means (solid lines) for the influence of different state predictors over the course of experimental rounds. The top row shows baseline switching probabilities across all situations in which participants observe (a) successful player(s), the following rows show deviations from this expectation on the logit scale.

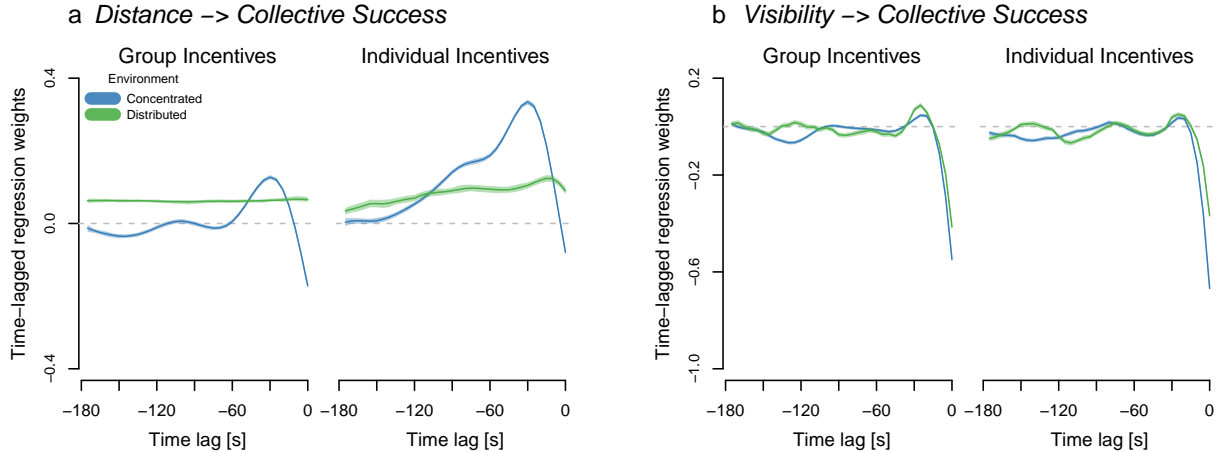


Figure S11. Collective visual-spatial dynamics for up to 3-minute time lags.

Time-lagged Gaussian-process regression weights (including 90% HPDIs) predicting collective foraging success (number of players exploiting a patch) based on (a) distance (average pairwise distance among players) and (b) visibility (number of visual connections among group members, ranging from 0, where no one is looking at others, and 12, where everyone is looking at everyone else) across different time intervals per incentive condition and environment.

REFERENCES

- Benhamou, S. (2004). How to reliably estimate the tortuosity of an animal's path:: straightness, sinuosity, or fractal dimension? *Journal of theoretical biology*, 229(2):209–220.
- Kitamura, T. and Imafuku, M. (2015). Behavioural mimicry in flight path of batesian intraspecific polymorphic butterfly papilio polytes. *Proceedings of the Royal Society B: Biological Sciences*, 282(1809):20150483.
- McLean, D. J. and Skowron Volponi, M. A. (2018). trajr: An r package for characterisation of animal trajectories. *Ethology*, 124(6):440–448.